The Journal of Prevention of Alzheimer's Disease 12 (2025) 100252

Contents lists available at ScienceDirect

The Journal of Prevention of Alzheimer's Disease

journal homepage: www.elsevier.com/locate/tjpad

Original Article

Plasma p-tau217 predicting brain-wide tau accumulation in preclinical AD

Hasom Moon, Xi Chen*, for the Alzheimer's Disease Neuroimaging Initiative[1]

Department of Psychology, Stony Brook University, Stony Brook, NY 11794, USA

ARTICLE INFO

Keywords:
Aβ PET
Longitudinal
p-tau217
Preclinical AD
Tau PET

ABSTRACT

Background: Recently developed blood test of Alzheimer's disease (AD) has been recognized as a promising alternative to CSF and PET, as it is noninvasive, cost-effective, and more accessible. Particularly, plasma p-tau217 shows high sensitivity in detecting β-amyloid (Aβ) and tau positivity in early AD. However, the potential value of p-tau217 in revealing Aβ and tau distribution and predicting future development has not been studied.
Objectives: We investigated the dose-response associations between p-tau217 and regional Aβ and tau measured by PET, as well as the longitudinal prediction of p-tau217 for prospective Aβ and tau accumulation measured by longitudinal PET.
Design: Cross-sectional and longitudinal analyses.
Setting: We used data in Anti-Amyloid Treatment in Asymptomatic Alzheimer's disease (A4) study ($N = 333$) for primary analyses and Alzheimer's Disease Neuroimaging Initiative (ADNI) ($N = 410$) for validation.
Participants: Cognitively unimpaired older adults ($N = 333$) from A4 study and cognitively unimpaired older adults ($N = 222$), mild cognitive impairment ($N = 114$), and dementia ($N = 74$) from ADNI.
Measurements: Plasma p-tau217 was measured using Lilly (A4) and Fujirebio (ADNI) assays. $^{18\text{-F}}$Florbetapir PET and $^{18\text{-F}}$Flortaucipir PET measured regional Aβ and tau.
Results: Plasma p-tau217 was associated with concurrent Aβ in most cortical regions and tau in temporo-parietal cortices. Longitudinally, p-tau217 predicted brain-wide tau accumulation in widespread cortical regions in preclinical AD, but not Aβ change anywhere.
Conclusions: Plasma p-tau217 shows dose-response, brain-wide relationships with concurrent Aβ and future tau development in preclinical AD, suggesting its potential in disease trajectory monitoring and large-scale screening for individuals approaching certain biological stages of AD in clinical trials.

1. Introduction

Extracellular deposition of β-amyloid (Aβ) plaques and intracellular aggregation of hyperphosphorylated tau proteins in neurofibrillary tangles are the hallmark pathologies of Alzheimer's disease (AD) [1–3]. Positron emission tomography (PET) and cerebrospinal fluid (CSF) provide in-vivo measurements of AD pathology that allow for clinical diagnosis of AD and can detect Aβ and tau even prior to significant symptoms [4]. Recently, blood-based biomarkers have emerged as a promising alternative that is more cost-effective, accessible, and less invasive [5,6]. In particular, plasma phosphorylated-tau (p-tau) biomarkers can differentiate AD from non-AD patients and show high correlations with AD pathologies in both autopsy-confirmed and PET-based AD studies [7–11]. Very recently, FDA approved the first blood test for AD using p-tau217/β-amyloid 1–42 ratio, recognizing that p-tau217 signals AD pathology with high accuracy and sensitivity [12–14] comparable to other previously FDA-approved CSF biomarkers [15–17].

Recent AD research and clinical trials have shown encouraging outcomes in treating mildly impaired individuals [18,19] and suggested that intervening before symptoms may be more optimal to prevent irreversible cognitive impairment [20]. In this coming era of disease-modifying treatments, blood-based biomarkers have the potential to enable large-scale pre-screening of individuals with preclinical AD pathology, particularly in areas with limited PET access, mitigating health disparities by enrolling underserved populations while reducing unnecessary PET scans [21].

While plasma p-tau biomarkers have drawn increasing attention, PET scans of Aβ and tau, as the gold standard for characterizing AD neuropathology, provide critical regional quantifications of pathology in the brain [22]. This unique information on spatial distribution of

* Corresponding author at: Department of Psychology, Stony Brook University, Stony Brook, NY 11794, USA.
E-mail address: xi.chen.8@stonybrook.edu (X. Chen).

[1] Data used in preparation of this article were obtained from the Alzheimer's Disease Neuroimaging Initiative (ADNI) database (adni.loni.usc.edu). As such, the investigators within the ADNI contributed to the design and implementation of ADNI and/or provided data but did not participate in the analysis or writing of this report. A complete listing of ADNI investigators can be found at: http://adni.loni.usc.edu/wp-content/uploads/how_to_apply/ADNI_Acknowledgement_List.pdf

https://doi.org/10.1016/j.tjpad.2025.100252
Received 10 March 2025; Received in revised form 5 June 2025; Accepted 13 June 2025

pathology has been increasingly recognized as an important aspect for understanding heterogeneity [23] and monitoring disease progression in AD [5]. Particularly, the regional presentation of tau reflects the biological staging of AD [24,25] and is closely predictive of downstream neurodegeneration (e.g., atrophy, hypometabolism) [26,27] and domain-specific cognitive impairment in AD [28–30], thus informing AD severity and predicting clinical manifestation. This valuable topographic information of tau captured by PET is unavailable in biofluid biomarkers. In this study, we investigate whether plasma p-tau217 can be used to infer regional burden and predict accumulation of AD pathology, especially tau, in preclinical AD by examining the dose-response relationships, cross-sectionally and longitudinally, between plasma p-tau217 and PET-quantified Aβ and tau.

Plasma p-tau217 has been related to signaling Aβ positivity and higher Aβ in precuneus, medial frontal, and temporal regions in cognitively unimpaired and impaired groups [31–34], with a weaker association in later disease stages [35]. Plasma p-tau217 has also been recently correlated with tau in limited temporal regions in earlier AD and broader temporo-parietal regions, further extending to frontal lobe, in later stages [31,32,35]. Researchers also found plasma p-tau217 increased in PET-confirmed Aβ and tau positive individuals in three different cohorts, further validating its value in estimating PET-based pathology [36]. Meanwhile, there is very limited investigation on how plasma p-tau217 can predict longitudinal change in PET. A few studies using BioFINDER data [37–39] found significant predictions of p-tau217 on early tau regions, suggesting the potential of plasma p-tau217 in predicting future tauopathy. Our study, building on the knowledge of the validity of plasma p-tau217, further examines its predictive utility for Aβ and tau pathologies at regional level particularly in preclinical AD.

Despite the preliminary evidence on cross-sectional associations, very little information is available on the predictive utility of p-tau biomarkers for longitudinal accumulation, especially in cognitively unimpaired people at preclinical stage where regional burden is most variable and the use of plasma biomarker is most valuable. Thus, the primary focus of this study was to explore how well plasma p-tau217 can reflect regional AD pathology in preclinical AD, using baseline plasma p-tau217 and longitudinal PET data from the Anti-Amyloid Treatment in Asymptomatic Alzheimer's disease (A4) study. In addition, we replicated our analyses in Alzheimer's Disease Neuroimaging Initiative (ADNI) for validation, where an independent sample and a different p-tau217 assay were used, to examine whether our conclusions were generalizable. We hypothesized that high plasma p-tau217 would be an indicator of globally elevated Aβ and increased tau burden in early-tau regions in the temporal lobe, and a valid predictor of longitudinal tau accumulation in preclinical AD. Specifically, p-tau217 would predict longitudinal tau accumulation in more neocortical regions, than the cross-sectional associations, as tau begins to spread beyond the temporal cortex in the development of AD, which can be predicted by elevations in p-tau217. Significant relationships between p-tau217 and regional AD pathology would suggest its unique value in informing early-stage AD and predicting future tau development especially when PET is not available.

2. Methods

2.1. Participants

This study included 333 Aβ+ cognitively unimpaired older adults (age 65–85 years) from the A4 study who had baseline plasma p-tau217, Aβ PET with $^{18\text{-}F}$Florbetapir (FBP) and tau PET with $^{18\text{-}F}$Flortaucipir (FTP). The details have been published elsewhere [20,40,41]. Briefly, participants were Aβ+ cognitively unimpaired older individuals, defined as CDR of 0, MMSE of 25–30, and Logical Memory IIA (delayed recall) of 6–18. Aβ status was determined by combining quantitative criteria and qualitative visual read. Tau PET was acquired for a subset of them.

In A4 study, the cross-sectional analysis included pre-randomization data at baseline from all participants including the anti-amyloid treatment and placebo groups. For the longitudinal analysis, we focused on the placebo group, including 138 with longitudinal FBP PET and 146 with longitudinal FTP PET. Meanwhile, we repeated all cross-sectional and longitudinal analyses in the two groups separately to examine any group-specific difference, and the primary results were largely consistent.

For validation and sensitivity analyses, 410 older adults with plasma p-tau217 from ADNI who underwent either Aβ PET with FBP (N = 410) or tau PET with FTP (N = 292) were included. Among them, 214 individuals were Aβ+ and 196 individuals were Aβ- based on ADNI's Aβ positivity threshold SUVR=1.11 (centiloid=19.76) [42]. For validation, we focused on the Aβ+ cognitively unimpaired group. For further sensitivity analysis, we examined all groups encompassing Aβ- participants and Aβ+ cognitively impaired group. Cross-sectional analyses included 410 participants with FBP PET and 291 participants with FTP PET. Longitudinal analyses only included participants with longitudinal prospective FBP (N = 133) or FTP PET (N = 76) scans after p-tau217 measurement. We note that the primary analyses (see Statistical Analysis for details) excluded participants with missingness in covariates such as APOE genotype information (Table 1) leading to a slightly smaller sample size. Data used in the preparation of this article were obtained from the ADNI database (adni.loni.usc.edu). The ADNI was launched in 2003 as a public-private partnership, led by Principal Investigator Michael W. Weiner, MD. The original goal of ADNI was to test whether serial magnetic resonance imaging (MRI), PET, other biological markers, and clinical and neuropsychological assessment can be combined to measure the progression of MCI and early AD. The current goals include validating biomarkers for clinical trials, improving the generalizability of ADNI data by increasing diversity in the participant cohort, and providing data concerning the diagnosis and progression of AD to the scientific community. For up-to-date information, see adni.loni.usc.edu.

To assess the cross-sectional associations between plasma p-tau217 and regional AD pathologies, we focused on concurrent PET closest to (within 1 year) the plasma p-tau217 exam date. To assess the longitudinal prediction of plasma p-tau217 on regional accumulation of AD pathologies, we focused on prospective change in PET using scans close to (within 1 year) and after the plasma p-tau217 exam date.

2.2. Plasma p-tau217

The details of plasma p-tau217 in A4 [43] and ADNI [44,45] have been published previously. Briefly, in A4 study, p-tau217 levels were measured using an electrochemiluminescence (ECL) immunoassay developed by Eli Lilly. The sample preparation was automated by the Tecan Fluent workstation, and the detection was performed on the MesoScale (MSD) Sector S Imager 600 MM at the CAP-accredited and CLIA-certified Lilly Clinical Diagnostics Laboratory. In ADNI, p-tau217 levels were analyzed on the Fujirebio Lumipulse G1200 automated immunoassay platform.

2.3. PET

PET data acquisition and processing in A4 [20,40,41] and ADNI [42,46] have been detailed previously. Briefly, in A4 study, FBP SUVR was normalized by whole cerebellum as the reference region. The composite summary SUVR was based on frontal, temporal, parietal, precuneus, anterior cingulate, and posterior cingulate cortices, and centiloid value was used for global Aβ (FBP centiloid = 183.07 * composite summary SUVR – 177.26). Additionally, we used frontal, temporal, parietal, precuneus, anterior cingulate, and posterior cingulate cortices as representative ROI SUVRs. FTP SUVR was normalized by cerebellar crus as the reference region. We used cortical ROI SUVRs and the early-tau composite (amygdala, entorhinal, and parahippocampal) provided in A4 study protocol [20].

In ADNI, we used FBP and FTP PET data with a 6 mm Gaussian Kernel. FBP SUVR was normalized by whole cerebellum as a refer-

Table 1
Characteristics and longitudinal PET visit information of participants in A4 and ADNI. The values are presented as mean ± standard deviation and number (%) for continuous and categorical variables, respectively. Among 410 participants from ADNI, 410 had Aβ PET that was used to define their Aβ positivity whose baseline characteristics are presented separately (214 Aβ+, 196 Aβ-). Among them, 291 had cross-sectional tau PET, 133 had longitudinal Aβ PET, and 76 had longitudinal tau PET.

	A4			ADNI			
	Total (N = 333)	Treatment (N = 165)	Placebo (N = 168)	Total (N = 410)	Aβ+(N = 214)	Aβ+ CU (N = 86)	Aβ-(N = 196)
Age	72.2 ± 4.8	72.6 ± 4.7	71.8 ± 4.9	75.1 ± 8.6*	76.5 ± 8.0†	76.1 ± 7.3‡	73.6 ± 8.9
Sex (female)	190 (57.1 %)	87 (52.7 %)	103 (61.3 %)	202 (49.3 %)*	105 (49.1 %)	59 (68.6 %)	97 (49.5 %)
Education	16.2 ± 2.9	16.4 ± 2.8	16.0 ± 2.9	16.4 ± 2.6	16.3 ± 2.8	16.6 ± 2.9	16.6 ± 2.3
APOE ε4 carrier (%)	194 (58.3 %)	95 (57.6 %)	99 (59.0 %)	165 (42.9 %)*	126 (62.4 %)	48 (67.9 %)	39 (21.3 %)
CDR Global	0 ± 0	0 ± 0	0 ± 0	0.3 ± 0.4*	0.4 ± 0.5†	0 ± 0.1	0.2 ± 0.3
CDR Sum of boxes	0.1 ± 0.2	0.1 ± 0.2	0.1 ± 0.2	1.5 ± 2.5*	2.2 ± 2.9†	0.1 ± 0.2	0.7 ± 1.5
MMSE	28.6 ± 1.3	28.7 ± 1.3	28.6 ± 1.3	27.0 ± 3.9*	25.8 ± 4.6†	28.8 ± 1.5	28.4 ± 2.4
FBP PET (centiloid)	65.6 ± 31.5	65.8 ± 32.1	65.4 ± 31.1	42.1 ± 51.3*	82.4 ± 39.3†	63.6 ± 34.5	−1.9 ± 10.6
P-tau 217 Lilly (U/ml)	0.28 ± 0.15	0.29 ± 0.16	0.27 ± 0.14				
P-tau 217 Fujirebio (pg/ml)				0.33 ± 0.35	0.50 ± 0.38	0.29 ± 0.21	0.14 ± 0.18
FBP PET visits	1–2			1–7			
Concurrent FBP PET – p-tau 217 interval (years)	−0.17 ± 0.06 [−0.52, −0.05]			−0.10 ± 0.32 [−1.00, 0.84]			
FBP PET follow-up intervals (years)	4.75 ± 0.84 [0.61, 6.40]			2.31 ± 0.72 [0.97, 5.73]			
FTP PET visits	1–5			1–4			
Concurrent FTP PET – p-tau 217 interval (years)	−0.04 ± 0.04 [−0.21, 0.14]			0.03 ± 0.17 [−0.95, 0.96]			
FTP PET follow-up intervals (years)	1.67 ± 0.46 [0.55, 6.78]			2.06 ± 1.40 [0.64, 5.98]			

* $p < .05$ A4 vs. ADNI total.
† $p < .05$ A4 vs. ADNI Aβ+.
‡ $p < .05$ A4 vs. ADNI Aβ+ CU.

ence region. The cortical summary SUVR was based on frontal, anterior/posterior cingulate, lateral parietal, lateral temporal regions, and centiloid value was used for global Aβ (FBP centiloid = 188.22 * cortical summary SUVR – 189.16). Additionally, we examined associations between p-tau217 and regional Aβ in cortical ROIs. FTP SUVR was normalized by inferior cerebellar GM as a reference region. We used cortical ROI SUVRs, as well as the temporal meta-ROI provided by ADNI [47].

2.4. Statistical analysis

To compare demographic and clinical characteristics of A4 and ADNI participants, *t*-test and chi-square test were used for continuous and categorical variables, respectively. Linear regression was used to present the associations between plasma p-tau217 and AD pathologies assessed by PET, adjusting for age, sex, and APOE ε4 carriership. Standardized regression coefficients (β) as well as unstandardized regression coefficients (b) and 95 % confidence interval (CI) were reported. Additionally, simple regression models presenting the bivariate relationships between p-tau217 and AD pathologies without any covariate were performed and included in the supplementary material. Statistical significance was reported based on p-values (< 0.05) after family-wise error (FWE) correction. Uncorrected p-values were included to help interpretations.

To highlight the potential utility of p-tau217 in inferring regional FTP SUVR, we visually compared the observed and estimated patterns of FTP PET. The observed pattern was calculated by averaging the regional SUVR of individuals who fell within the specific range of p-tau217. To visualize the estimated pattern of concurrent tau distribution and future tau accumulation, we used unstandardized regression coefficients (b) in the regression model for each ROI, ($y \sim b_0 + b_1 \bullet$p-tau217 $+ b_2 \bullet$age $+ b_3 \bullet$sex $+ b_4 \bullet$APOE ε4 carriership), to calculate estimated value (i.e., estimated ROI SUVR for cross-sectional, estimated slope of ROI SUVR for longitudinal) for a given p-tau217 while keeping other covariates constant at the mean value in the sample (mean age, proportion of female, proportion of ε4 carrier). We combined the last four groups with highest p-tau217 (0.6 to 1.0 U/ml). The number of participants in these groups was much smaller ($n < 8$). This allows us to create a relatively equal distribution with a sample size comparable to other lower groups. To identify regions approaching tau-positivity given different p-tau217 levels, we used two cut-offs (SUVR=1.22 [48] and 1.29 [49]) to define tau-positive regions.

To analyze longitudinal prediction, linear mixed effects models (LMM) were used to extract random slopes for longitudinal changes in PET per year, allowing each individual to have a unique slope. Specifically, simple LMM included the time interval (years) between baseline plasma p-tau217 exam date and each scan date as a fixed predictor and estimated both random intercept and random slope. The fixed slope (average slope of the group) and random slope (individual deviance from the average slope) together represents the individual slope. The A4 study included only two Aβ PET visits for every participant. Thus the slopes for longitudinal Aβ PET changes in A4 were calculated using the following formula: Individual slope of Aβ PET changes = ($SUVR_{follow\text{-}up}$ – $SUVR_{baseline}$) / time differences in years. All statistical analyses were performed using R version 4.4.1.

3. Results

3.1. Demographic and clinical characteristics of participants in A4 and ADNI

Participants characteristics at baseline are presented in Table 1. The A4 study included all Aβ+ cognitively unimpaired older individuals, while 214 (52.2 %) participants were Aβ+ in ADNI across different clinical stages. Compared to ADNI, A4 study participants were younger ($t = -5.903$, $p < .001$) and had a higher proportion of females ($x^2 = 4.166$, $p = .041$) and APOE ε4 carriers ($x^2 = 16.331$, $p < .001$). ADNI participants were clinically more advanced than A4, including 222 cognitively unimpaired, 114 MCI, and 74 dementia patients.

Overall, A4 participants (65.6 centiloid) showed higher global Aβ than ADNI (42.1 centiloid) which included both Aβ- and Aβ+ participants ($t = 7.670$, $p < .001$). ADNI Aβ+ (86 cognitively unimpaired and 128 cognitively impaired) participants (82.4 centiloid) had higher global Aβ than A4 ($t = -5.241$, $p < .001$), and there was no signifi-

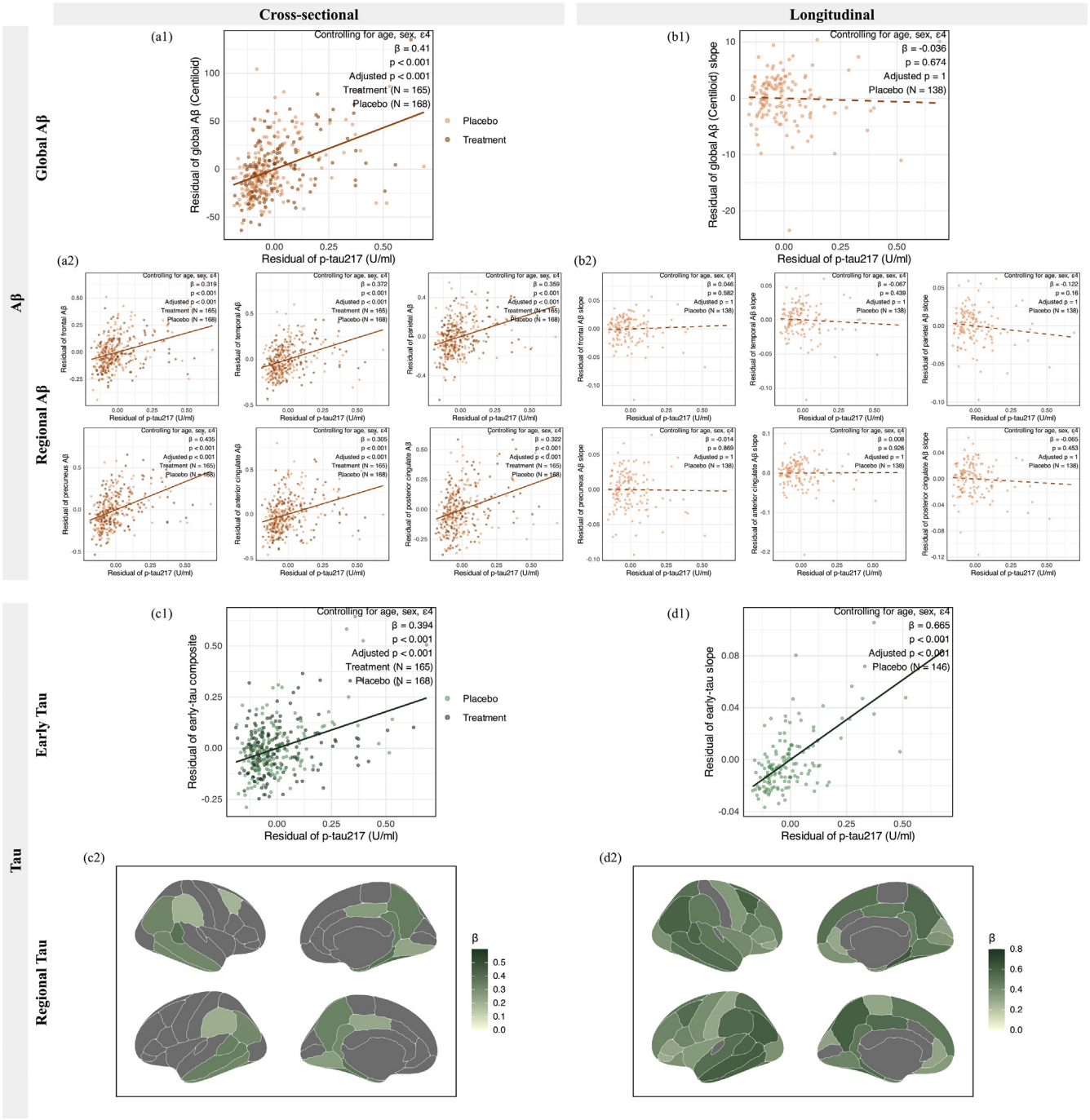

Fig. 1. Relationships between p-tau217 and PET in A4 after adjusting for age, sex, and APOE status. (**a**) P-tau217 was significantly associated with cross-sectional Aβ levels globally (**a1**) and at regional level (**a2**) ($p_{FWE} < 0.05$), **(b)** but did not predict longitudinal Aβ changes at the global (**b1**) nor regional level (**b2**) ($p_{FWE} > 0.05$). **(c)** P-tau217 was significantly associated with cross-sectional tau deposition in the early-tau composite region (**c1)** and in temporo-parietal regions including fusiform gyrus, banks of the superior temporal sulcus, parahippocampal gyrus, entorhinal cortex, precuneus, isthmus cingulate cortex, middle temporal gyrus, inferior parietal lobule, inferior temporal gyrus, posterior cingulate cortex, lingual gyrus, supramarginal, and caudal middle frontal gyrus (**c2**) ($p_{FWE} < 0.05$). **(d)** P-tau217 was significantly associated with longitudinal changes in tau accumulation in the early-tau composite region (**d1**) and in most cortices including temporal, parietal, frontal, and occipital regions (**d2**) ($p_{FWE} < 0.05$).

cant difference in centiloid levels between A4 and ADNI Aβ+ cognitively unimpaired participants (63.6 centiloid) ($t = 0.481$, $p = .631$). Additionally, when compared to ADNI Aβ+ or ADNI Aβ+ cognitively unimpaired, A4 study participants remained younger ($t = -7.192$ and -4.698, respectively; both $p < .001$), although there were no significant differences in sex ($x^2 = 3.035$, $p = .081$ and $x^2 = 3.316$, $p = .069$, respectively) and APOE ε4 carriership ($x^2 = 0.724$, $p = .395$ and $x^2 = 0.001$, $p = .970$, respectively).

3.2. Cross-sectional and longitudinal relationships between plasma p-tau217 and Aβ PET in A4

Cross-sectionally, higher p-tau217 was related to greater concurrent global Aβ ($\beta = 0.410$, $b = 86.477$, 95 % CI = 66.540 – 106.415, $p_{FWE} < 0.001$; Fig. 1a1) and regional Aβ in all cortical composite ROIs ($\beta = 0.305 – 0.435$, $b = 0.355 – 0.664$, all $p_{FWE} < 0.001$; Fig. 1a2) with the strongest correlation observed in precuneus ($\beta = 0.435$, $b = 0.664$,

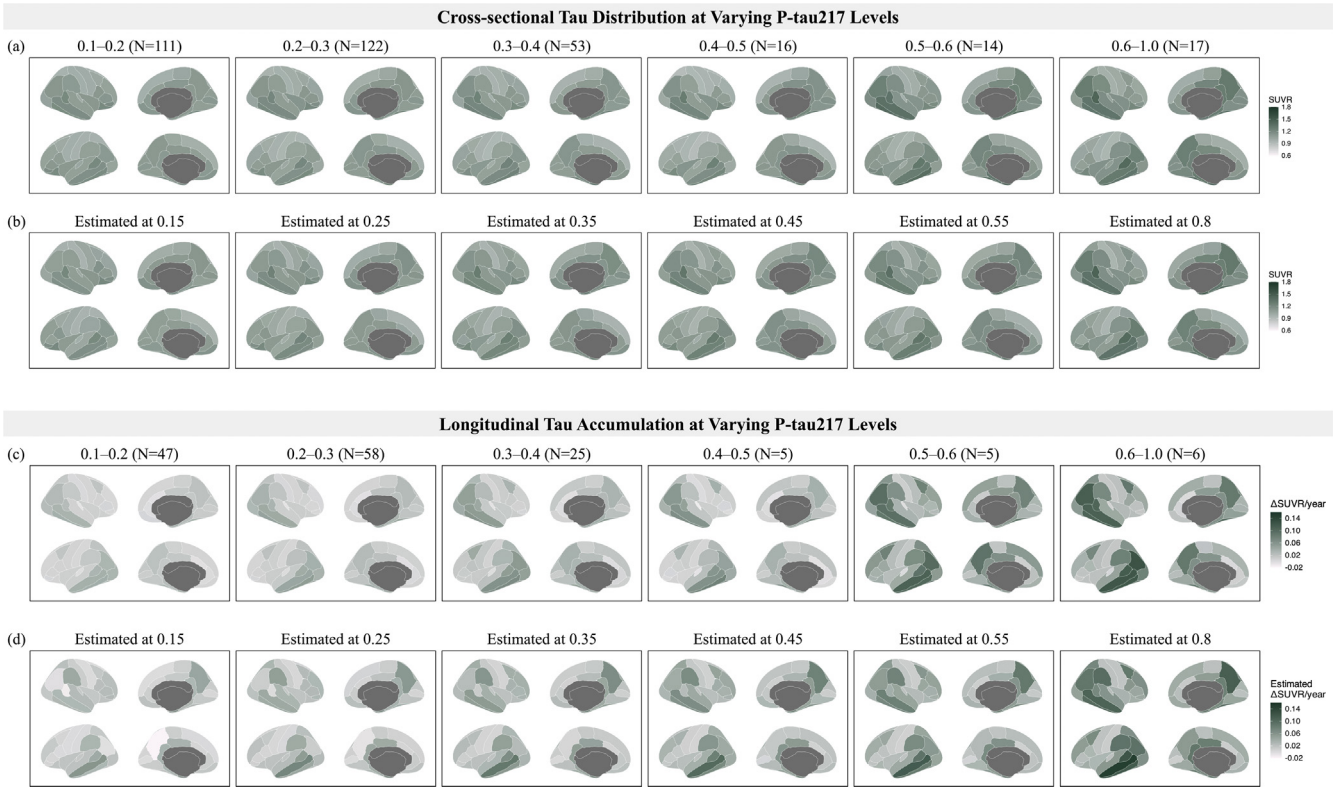

Fig. 2. High similarities between the observed and estimated regional tau PET pattern across the levels of p-tau217 (U/ml). (a) observed and **(b)** estimated concurrent tau deposition. **(c)** observed and **(d)** estimated longitudinal changes in tau accumulation. We used unstandardized regression coefficient (b) in the regression model for each ROI, ($y \sim b_0 + b_1$•p-tau217 + b_2•age + b_3•sex + b_4•APOE ε4 carriership), to calculate estimated value (i.e., estimated ROI SUVR for cross-sectional, estimated slope of ROI SUVR for longitudinal) for a given p-tau217 while keeping other covariates constant at the mean value in the sample.

95 % CI = 0.519 – 0.809, $p_{FWE} < 0.001$). Longitudinally, p-tau217 was not predictive of global Aβ slope ($\beta = -0.036$, $b = -1.223$, 95 % CI = −6.960 – 4.515, $p = .674$; Fig. 1b1) nor regional Aβ in any ROIs ($\beta = -0.122 – 0.046$, $b = -0.022 – 0.009$, all $p > .05$; Fig. 1b2). The bivariate relationships between p-tau217 and Aβ PET without covariates are very consistent with the full model results and presented in Supplementary Fig. 1.

Repeating the cross-sectional analyses separately in two groups, we found that the cross-sectional results were very similar across treatment and placebo groups, consistent with the strong relationship reported in the whole group (Supplementary Fig. 2a). Longitudinally, when repeating the analysis in the treatment group, we found that individuals with higher baseline p-tau217 had greater Aβ decrease in anterior cingulate ($\beta = -0.238$, $b = -0.054$, 95 % CI = −0.092 – −0.016, $p_{FWE} = 0.040$; Supplementary Fig. 2b), suggesting that participants in the treatment group with higher p-tau217 at baseline benefited most from the anti-amyloid treatment with the larger decrease in Aβ. However, when further examining a moderation effect of treatment on the relationship between p-tau217 and longitudinal Aβ slope, there was no significant group difference in the relationship (all $p > .05$).

3.3. Cross-sectional and longitudinal relationships between plasma p-tau217 and tau PET in A4

Cross-sectionally, higher p-tau217 was related to greater concurrent tau deposition in the early-tau composite region ($\beta = 0.394$, $b = 0.358$, 95 % CI = 0.267 – 0.449, $p_{FWE} < 0.001$; Fig. 1c1). Specifically, higher p-tau217 was indicative of greater tau mostly in temporo-parietal regions including fusiform, banks of the superior temporal sulcus, parahippocampal, entorhinal, precuneus, isthmus cingulate, middle temporal, inferior parietal, inferior temporal, lingual, and posterior cingulate, supramarginal, caudal middle frontal ROIs ($\beta = 0.192 – 0.396$, $b = 0.149 – 0.434$, $p_{FWE} < 0.05$; Fig. 1c2). Longitudinally, higher p-tau217 was predictive of faster tau accumulation in the early-tau composite region ($\beta = 0.665$, $b = 0.123$, 95 % CI = 0.100 – 0.146, $p_{FWE} < 0.001$; Fig. 1d1) and faster tau accumulation in broader regions extending to the majority of cortical regions beyond temporo-parietal regions ($\beta = 0.278 – 0.619$, $b = 0.016 – 0.147$, $p_{FWE} < 0.05$; Fig. 1d2) in both hemispheres. The bivariate relationships between p-tau217 and tau PET are similar and presented in Supplementary Fig. 3.

Repeating the analyses in both groups yielded similar results across the treatment and the placebo groups with slightly stronger relationships in the placebo group than the treatment group for both cross-sectional associations (Supplementary Fig. 4a) and longitudinal predictions (Supplementary Fig. 4b). However, the result patterns are overall very consistent, suggesting the reliable predictive utility of p-tau217 for tau PET.

3.4. Estimating regional tau deposition, accumulation, and positivity using plasma p-tau217

To further aid the interpretation of our results, we explored the potential use of p-tau217 to [1] estimate the concurrent distribution and future accumulation of tau, and [2] identify regions approaching tau-positive. We first developed regression models for each region where regional tau SUVR was estimated using p-tau217 and the covariates. We observed high similarities in regional tau patterns between the observed PET data and estimated tau SUVRs across p-tau217 levels, in both concurrent regional tau deposition (Fig. 2a–b) and longitudinal regional tau accumulation (Fig. 2c–d), suggesting high predictive utility of p-tau217 for regional tau. For example, people with 0.55 U/ml of p-tau217 are likely to have elevated tau in medial, lateral, and middle temporal re-

Table 2
Estimated regional tau-positivity using different SUVR cut-offs: (a) 1.22 and (b) 1.29. Each estimated SUVR was calculated using unstandardized regression coefficients from regression model ($y \sim b_0 + b_1$•p-tau217 $+ b_2$•age $+ b_3$•sex $+ b_4$•APOE $\varepsilon 4$ carriership) with substituting the given p-tau217 and keeping other covariates constant at the mean value in the sample (mean age, proportion of female, proportion of $\varepsilon 4$ carrier.

(a) When using 1.22 SUVR to define regional tau positivity (Maass et al., 2017), some temporal regions (e.g., banks of the superior temporal sulcus, entorhinal, fusiform) start to reach the tau positive threshold at 0.25–0.35 of p-tau217, followed by other temporal and medial parietal regions (e.g., inferior temporal, middle temporal, parahippocampal, precuneus) at 0.45–0.55 of p-tau217, parietal regions (e.g., inferior parietal, isthmus cingulate, temporal pole, posterior cingulate) at 0.65–0.85 of p-tau217, and additional occipital regions (e.g., lingual) at 0.95 of p-tau217.

Level of p-tau217 (U/ml)	Estimated tau-positive regions (SUVR ≥ 1.22)
0.15	
0.25	right bankssts, left bankssts, right entorhinal
0.35	+ right fusiform, left entorhinal
0.45	+ right inferior temporal, left middle temporal, left fusiform, right middle temporal, left inferior temporal
0.55	+ left parahippocampal, right precuneus, right parahippocampal
0.65	+ left inferior parietal, right inferior parietal
0.75	+ right isthmus cingulate, left precuneus, left temporal pole
0.85	+ right posterior cingulate, left isthmus cingulate
0.95	+ right temporal pole, left lingual

(b) When a more rigorous cut-off of 1.29 SUVR was used to define tau positivity in each region (Lowe et al., 2019), medial and lateral, inferior temporal regions (banks of the superior temporal sulcus, entorhinal, fusiform) become tau-positive at 0.45–0.55 U/ml of p-tau 217, followed by broader temporal and medial parietal regions (inferior temporal, middle temporal, parahippocampal, precuneus) at 0.65–0.75, before extending to parietal regions approaching positive (inferior parietal, isthmus cingulate) at 0.95.

Level of p-tau217 (U/ml)	Estimated tau-positive regions (SUVR ≥ 1.29)
0.15	
0.25	
0.35	
0.45	right bankssts, right entorhinal, left bankssts
0.55	+ left entorhinal, right fusiform
0.65	+ right inferior temporal, left fusiform, left middle temporal, right middle temporal
0.75	+ left inferior temporal, left parahippocampal, right parahippocampal, right precuneus
0.85	
0.95	+ right inferior parietal, left inferior parietal, right isthmus cingulate

gions as well as inferior parietal and posterior medial regions (Fig. 2b), with several temporal regions including banks of the superior temporal sulcus, entorhinal, fusiform, inferior and middle temporal cortices, parahippocampal, and precuneus approaching positive using cut-off of 1.22 SUVR (Table 2a). It suggests that this individual has positive PET signals in Braak Stage IV regions, likely having even later Braak stage tau pathology if inspected in an autopsy [50,51]. Meanwhile, they are expected to accumulate approximately 0.07 SUVR per year in inferior temporal, middle temporal, and inferior parietal regions (Fig. 2d). In the visualizations, the four groups at higher end of p-tau217 were combined into one group (0.6 – 1.0 U/ml of p-tau217) to create a relatively equal distribution with a sample size comparable to the other lower groups and to mitigate bias that the small number of participants per group leads to greater variability.

3.5. Plasma p-tau217 and PET relationships in ADNI

3.5.1. Validation in Aβ+ cognitively unimpaired group

In Aβ+ cognitively unimpaired group, higher p-tau217 was related to greater cross-sectional global Aβ (β = 0.485, b = 80.098, 95 % CI = 46.338 – 113.857, $p_{FWE} < 0.001$; Fig. 3b1). Specifically, higher p-tau217 was indicative of greater Aβ in globally diffused cortical regions, including parietal, frontal, and temporal cortices (β = 0.382 – 0.541, b = 0.278 – 0.602, $p_{FWE} < 0.05$; Fig. 3b2). Longitudinally, p-tau217 appeared to predict longitudinal global Aβ accumulation, although the prediction was not significant after FWE correction (β = 0.499, b = 1.962, 95 % CI = 0.799 – 3.124, p = .002, p_{FWE} = 0.112; Fig. 3e1). Specifically, higher p-tau217 was associated with steeper Aβ accumulation in limited regions of right hemisphere, including paracentral, supramarginal, precuneus, posterior cingulate, fusiform, inferior temporal regions (β = 0.503 – 0.634, b = 0.009 – 0.018, $p_{FWE} < 0.05$; Fig. 3e2). Overall, the cross-sectional association of p-tau217 for global Aβ burden was consistent with the findings in A4 data of preclinical AD, while the longitudinal prediction of p-tau217 for regional Aβ were additionally observed in ADNI data.

When predicting tau PET, p-tau217 was related to cross-sectional temporal meta-ROI tau at a similar strength as observed in A4 (β = 0.394; Fig. 1c1), despite being non-significant after FWE correction (β = 0.333, b = 0.195, 95 % CI = 0.036 – 0.354, p = .017, p_{FWE} = 1; Fig. 3h1). Before FWE correction, higher p-tau217 was associated with greater tau deposition in similar regions as observed in A4, including inferior parietal, inferior temporal, fusiform, lateral occipital, lingual, and middle temporal regions (β = 0.304 – 0.380, b = 0.159 – 0.451, $p < .05$, $p_{FWE} > 0.05$; Supplementary Fig. 5), although these associations did not survive FWE correction. Longitudinally, different from A4, p-tau217 was not related to longitudinal tau accumulation in temporal meta-ROI (β = −0.102, b = −0.011, 95 % CI = −0.076 – 0.054, p = .725; Fig. 3k1) nor in any ROIs (all $p > .05$; Fig. 3k2 and Supplementary Fig. 5).

3.5.2. Sensitivity analysis in Aβ+ cognitively impaired and Aβ- groups

In Aβ+ cognitively impaired group, p-tau217 was strongly related to brain-wide tau burden and longitudinal tau accumulation. Specifically, higher p-tau217 was related to greater temporal meta-ROI tau (β = 0.582, b = 0.692, 95 % CI = 0.483 – 0.902, $p_{FWE} < 0.001$; Fig. 3i1) as well as greater brain-wide tau deposition in the majority of cortical regions (β = 0.367 – 0.706, b = 0.211 – 1.056, $p_{FWE} < 0.05$; Fig. 3i2), which encompass much broader regions than in A4. Longitudinally, p-tau217 was related to faster temporal meta-ROI tau accumulation (β = 0.887, b = 0.140, 95 % CI = 0.096 – 0.183, $p_{FWE} < 0.001$; Fig. 3l1) and steeper

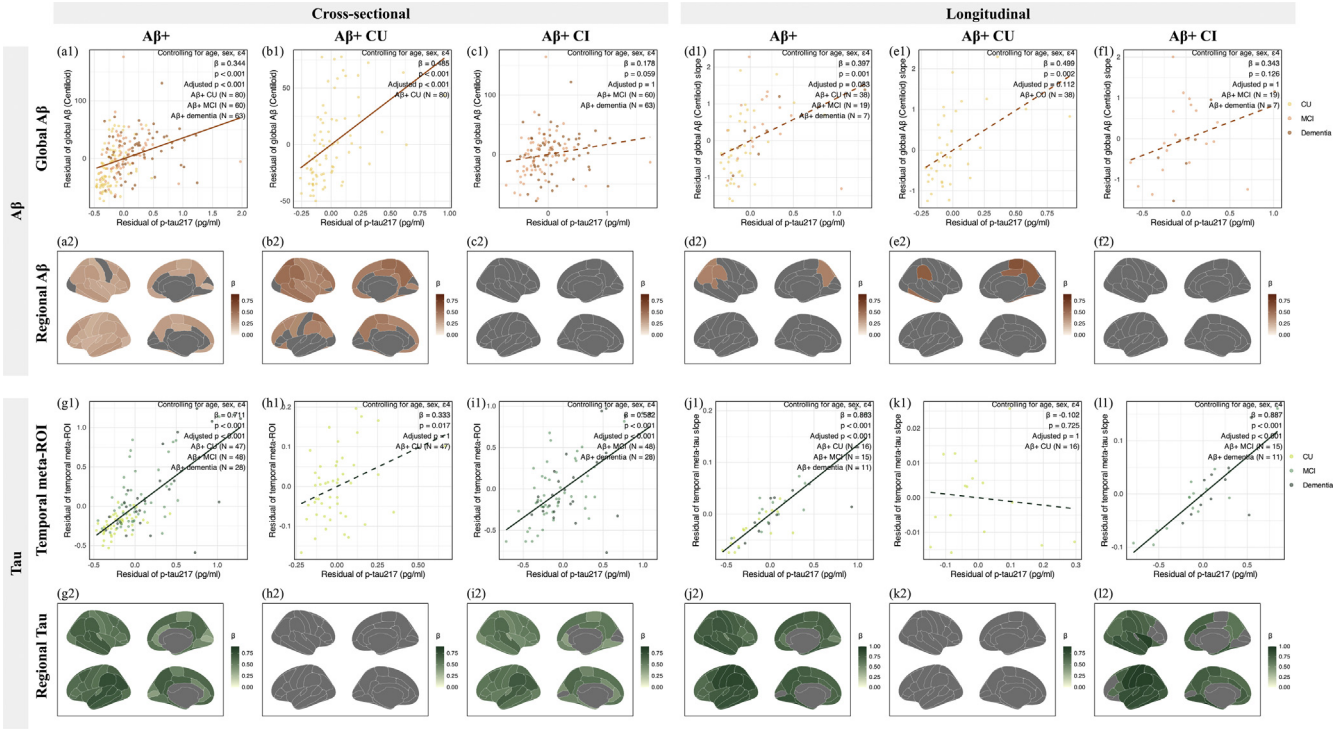

Fig. 3. Relationships between p-tau217 and PET in ADNI after adjusting for age, sex, and APOE status. P-tau217 was significantly associated with cross-sectional Aβ (**a1–2**) and tau (**g1–2**) levels and predicted longitudinal tau (**j1–2**), but not Aβ (**d1–2**), changes. In Aβ+ cognitively unimpaired group, p-tau217 was significantly associated with cross-sectional Aβ levels **(b1–2)** ($p_{FWE} < 0.05$) but did not predict longitudinal Aβ changes **(e1–2)** ($p_{FWE} > 0.05$). P-tau217 was not associated with concurrent temporal meta-ROI tau deposition **(h1–2)** ($p_{FWE} > 0.05$) nor longitudinal tau changes **(k1–2)** ($p_{FWE} > 0.05$). However, in Aβ+ cognitively impaired group, p-tau217 was strongly associated with concurrent temporal meta-ROI tau as well as brain-wide tau deposition in most regions **(i1–2)** ($p_{FWE} < 0.05$) and predicted longitudinal tau accumulation **(l1–2)** ($p_{FWE} < 0.05$), but not Aβ **(c1–2, f1–2)** ($p_{FWE} > 0.05$).

tau accumulation in most regions ($\beta = 0.600 – 0.960$, $b = 0.020 – 0.186$, $p_{FWE} < 0.05$; Fig. 3l2). Overall, cross-sectional association and longitudinal prediction of p-tau217 for brain-wide tau was observed in Aβ+ cognitively impaired group of ADNI, with much stronger and broader relationships than those in preclinical AD of A4 data. On the other hand, p-tau217 was not related to cross-sectional nor longitudinal Aβ in Aβ+ cognitively impaired individuals (all $p > .05$ in global Aβ, all $p_{FWE} > 0.05$ in any ROIs; Fig. 3c and 3f).

In Aβ- participants, there were no significant findings in global Aβ, temporal meta-ROI tau (both $p > .05$; Supplementary Fig. 6), or regional Aβ or tau SUVRs (all $p_{FWE} > 0.05$; Supplementary Fig. 6). The bivariate relationships between p-tau217 and Aβ and tau PET are similar and presented in Supplementary Fig. 7–8.

In summary, the associations between p-tau217 and PET observed in A4 data were overall well replicated in Aβ+ participants in ADNI. Interestingly, the association between p-tau217 and cross-sectional Aβ was driven by Aβ+ cognitively unimpaired individuals, which corresponded to preclinical AD in A4, while the cross-sectional association and longitudinal prediction of p-tau217 for brain-wide tau were more evident in Aβ+ cognitively impaired group.

4. Discussion

Plasma p-tau217 has emerged as a promising biomarker for AD. Although its value in identifying Aβ+ individuals has been increasingly recognized, its potential in indicating severity of regional Aβ and tau pathology in AD and predicting future AD pathology development is still unclear. In this study, we showed that in preclinical AD, plasma p-tau217 was highly indicative of Aβ burden across the brain but did not predict longitudinal Aβ change, while plasma p-tau217 closely reflected tau burden in temporo-parietal regions and predicted brain-wide tau accumulation in broader cortical regions across the brain. These findings advance our existing knowledge on the high accuracy of p-tau217 in inferring PET-based biomarkers [36,38] and suggest that elevations in plasma p-tau217 may reflect earlier tau change prior to PET detection in Alzheimer's disease and highlight the potential utility of plasma p-tau217 in indexing concurrent Aβ and early tau severity, as well as predicting future tau accumulation at regional level in the development of Alzheimer's disease.

In preclinical AD, higher p-tau217 was related to increased Aβ burden in many cortical regions, validating its use as a biomarker of Aβ severity. This was further replicated in ADNI where the cross-sectional associations with concurrent Aβ were driven by Aβ+ cognitively unimpaired participants, not Aβ- participants nor Aβ+ cognitively impaired group. This agrees with previous findings that p-tau217 was only related to global Aβ in Aβ+ and that there was lower or non-significant association in Aβ- people [33,52,53]. Our study further provides regional evidence that p-tau217 can further reflect Aβ deposition in preclinical AD and that these relationships are evident across the majority of cortical regions.

Higher p-tau217 also indicated tau deposition in temporo-parietal regions, primarily driven by Aβ+ participants. Its association pattern mirrors the stereotypical tau distribution in early-stage of AD [54]. When comparing the p-tau217 estimated tau map to the actual regional tau SUVR measured by PET (Fig. 2a–b), we observed high similarity suggesting the potential use of p-tau217 to estimate the likely distribution of brain tauopathy in asymptomatic individuals especially in typical AD cases. For example, individuals with elevated p-tau217 at 0.45 U/ml can be expected to have neocortical regions approaching PET-based tau positivity primarily in the temporal lobe (Table 2a), with the regions extending to the parietal lobe at 0.55 U/ml suggesting that this individual has positive PET signals in Braak Stage IV regions and may present even

later Braak stage tauopathy if inspected in an autopsy [50,51]. To our knowledge, only very few studies have explored the association between plasma biomarker and regional tau PET in preclinical AD, with findings of its association with advanced Braak stages [55–57]. Our findings suggest that p-tau217 can help offer information on the likely spatial extent of tau distribution in the brain, which is especially valuable when tau PET is not available.

Importantly, p-tau217 strongly predicted prospective tau accumulation measured by longitudinal PET in A4 participants. In particular, higher p-tau217 was related to steeper tau accumulation across many neocortical regions, expending beyond temporo-parietal regions where increasing tau is most characteristic in preclinical stage. Specifically, when inspecting the accumulation pattern of tau SUVR predicted by p-tau217 (Fig. 2d), higher p-tau217 predicts tau accumulation in medial, middle, and lateral temporal regions, then inferior and medial parietal regions, followed by frontal and association cortex, closely following the spreading pattern of tau in early AD. P-tau217 has previously been associated with tau PET in broader, later regions only in cognitively impaired individuals [31,32,35]. Our study presents that longitudinally, p-tau217 can predict subsequent tau accumulation in neocortical tau regions beyond medial temporal lobe as early as in cognitively unimpaired individuals. This suggests that p-tau217 may be used to sensitively identify individuals who likely present neocortical tauopathy or are accumulating neocortical tau, which can be especially helpful when enrolling participants approaching certain tau stages in clinical trials especially focusing on anti-tau treatment.

Meanwhile, we noted that p-tau217 was not predictive of regional tau increase in preclinical AD (Aβ+ cognitively unimpaired) in ADNI; instead, the prediction of p-tau217 for longitudinal tau was observed in later stages of AD continuum (Aβ+ cognitively impaired). Several factors may have contributed to the different observations. First, ADNI has a very small sample of preclinical AD with p-tau217 and longitudinal tau PET ($N = 16$) where we attempted the exact replication as in A4. This small number of participants greatly limited our analysis power. Second, the ADNI preclinical AD were at the lower end of p-tau217 with limited change (cool color; Supplementary Fig. 9), indicative of earlier stage of tauopathy, which may suggest that the prediction of p-tau217 for longitudinal tau changes would be reflective across AD continuum but less informative when tau change is minimal. Finally, the ADNI sample used a different assay of p-tau217. Although both assays have shown high accuracy for AD pathology, the Lilly assay used in A4 appears to have slightly better performance for detecting longitudinal change[58], which may contribute to the difference in the result. Nevertheless, the significant relationships with concurrent and longitudinal tau, but not Aβ, in the Aβ+ cognitively impaired group may suggest p-tau217 tracks tauopathy, but not Aβ, very well as Aβ may enter a plateau while tau continues to accumulate in more advanced stage of AD, confirming p-tau217 as a promising biomarker of subsequent tau accumulation.

Interestingly, despite the strong association with concurrent Aβ deposition in widespread regions, p-tau217 was not related to longitudinal Aβ accumulation in preclinical AD, which is largely replicated in ADNI. Previous studies have reported that plasma biomarkers of p-tau appeared more strongly associated with Aβ PET than tau [11,34], suspecting that its level reflects Aβ rather than increasing tau pathology. But we found in the present study that p-tau217 is primarily related to concurrent brain-wide Aβ deposition (but not tau) and longitudinal brain-wide tau change (but not Aβ). Phenomenally, the emergence of early tauopathy rises as Aβ deposition becomes detectable in Aβ PET, likely leading to the high correlation between p-tau217 and Aβ PET. We argue that the soluble form of p-tau217, despite being a useful proxy of Aβ, labels the pretangle of tauopathy before tau aggregates detected by tau PET [59] and thus sensitively predicts the development of neurofibrillary tangles that are closely associated with deposition of Aβ plaques. P-tau217, as a significant predictor of future tau aggregation, should be considered an early biomarker being abnormal prior to than PET [55]. However, its prediction for tau changes and the lack of prediction for Aβ changes should not hinder the use of p-tau217 as a marker for current Aβ. Future studies may investigate more waves of data including longitudinal p-tau217 change to examine whether elevations in p-tau217 may be closely related to changes in Aβ or tau PET change.

Overall, our study highlights that the significant potential of plasma p-tau217 in inferring the spatial extent of tau pathology, which reveals the severity and biological staging of the disease. The newly revised criteria for diagnosis and staging of Alzheimer's disease [2] highlights the role of plasma biomarker as a Core 1 biomarker providing diagnostic information suggesting AD positivity, and tau PET as a Core 2 biomarker providing prognostic information such as neocortical tau presence that defines biological staging of AD. The very recent FDA approval of the first blood test for AD marks the beginning of a new era for AD biomarkers. Our study suggests that a single measure of p-tau217 may have the potential of offering both the diagnostic information regarding Aβ positivity and also the estimated regional tau presence that can help determine a patient's biological staging when tau PET is not available.

While our study has many strengths, including the use of longitudinal PET, the validation of results in a different sample, and well-balanced sample distribution, including Aβ+ individual with low tau yet capturing full spectrum in the early stage of AD (Supplementary Fig. 10), it does have limitations. First, we replicated our analyses using ADNI data and found the primary findings in A4 study were supported. However, due to differences in plasma biomarker and tau PET processing pipelines, we were not able to directly examine if the exact critical values for plasma p-tau217 for regional tau positivity would be similar in a new sample. Previous studies showed that different assays of p-tau217 had relatively comparable accuracy for identifying AD pathology [60,61], but our findings should be further validated by the same assay of plasma p-tau217 and other assays for their generalizability. Nevertheless, most of the results found in A4 were largely replicated, demonstrating convergence across different assays. With increasing efforts in harmonizing PET biomarkers [62,63], future studies may explore a standardized scale for plasma p-tau217 concentrations, which would facilitate broader use and comparison of p-tau217 as a rising biomarker for AD. Additionally, the small sample size in ADNI also limited further explorations. The lack of sufficient phenotypical heterogeneity in impaired individuals did not allow further examination of how clinical phenotypes may help to improve regional-specific prediction of tauopathy. It should be noted that the revealed utility of p-tau217 in inferring regional tau largely relies on AD-related stereotypical tau pattern. Atypical variants of AD may have distinct tau distribution deviating from stereotypical one [28,64]. Future studies with larger samples in non-amnestic AD are needed to examine the use of p-tau217 in estimating tau distribution and spreading across different phenotypes. Similarly, the estimation and prediction based on p-tau217 are most appropriate to offer inferences at the group level, while individualized prediction would rely on much more individual variability information. Finally, the lack of sample diversity in existing AD research data may limit the generalizability of our findings. The samples in both cohorts are highly educated with mean education greater than 16 years. Future studies are needed to include participants from more diverse backgrounds.

In conclusion, our study underscores the role of plasma p-tau217 in informing concurrent Aβ and temporo-parietal tau burden, as well as predicting future tau accumulation at regional level, in cognitively unimpaired people developing AD. Plasma p-tau217 has significant potential in screening individuals approaching certain biological stages of AD, particularly offering inferences regarding the present and future of tauopathy. This can facilitate the enrollment in clinical trials targeting a specific pathology at a certain stage and also allow better monitoring of the disease progression.

Statement of informed consent

All human subjects provided written informed consent.

Funding

Preparation of the manuscript was supported by Stony Brook Research Funds.

Declaration of generative AI and AI-assisted technologies in the writing process

No generative AI and AI-assisted technologies are used in the wiring process.

Declaration of competing interest

The authors declare that they have no known competing financial interests or personal relationships that could have appeared to influence the work reported in this paper.

CRediT authorship contribution statement

Hasom Moon: Writing – original draft, Visualization, Validation, Software, Formal analysis. **Xi Chen:** Writing – review & editing, Supervision, Software, Conceptualization.

Acknowledgements

The A4 Study is a secondary prevention trial in preclinical Alzheimer's disease, aiming to slow cognitive decline associated with brain amyloid accumulation in clinically normal older individuals. The A4 Study is funded by a public-private-philanthropic partnership, including funding from the National Institutes of Health-National Institute on Aging, Eli Lilly and Company, Alzheimer's Association, Accelerating Medicines Partnership, GHR Foundation, an anonymous foundation and additional private donors, with in-kind support from Avid and Cogstate. The companion observational Longitudinal Evaluation of Amyloid Risk and Neurodegeneration (LEARN) Study is funded by the Alzheimer's Association and GHR Foundation. The A4 and LEARN Studies are led by Dr. Reisa Sperling at Brigham and Women's Hospital, Harvard Medical School and Dr. Paul Aisen at the Alzheimer's Therapeutic Research Institute (ATRI), University of Southern California. The A4 and LEARN Studies are coordinated by ATRI at the University of Southern California, and the data are made available through the Laboratory for Neuro Imaging at the University of Southern California. The participants screening for the A4 Study provided permission to share their de-identified data in order to advance the quest to find a successful treatment for Alzheimer's disease. We would like to acknowledge the dedication of all the participants, the site personnel, and all of the partnership team members who continue to make the A4 and LEARN Studies possible. The complete A4 Study Team list is available on: www.actcinfo.org/a4-study-team-lists. Data collection and sharing for the Alzheimer's Disease Neuroimaging Initiative (ADNI) is funded by the National Institute on Aging (National Institutes of Health Grant U19AG024904). The grantee organization is the Northern California Institute for Research and Education. In the past, ADNI has also received funding from the National Institute of Biomedical Imaging and Bioengineering, the Canadian Institutes of Health Research, and private sector contributions through the Foundation for the National Institutes of Health (FNIH) including generous contributions from the following: AbbVie, Alzheimer's Association; Alzheimer's Drug Discovery Foundation; Araclon Biotech; BioClinica, Inc.; Biogen; Bristol-Myers Squibb Company; CereSpir, Inc.; Cogstate; Eisai Inc.; Elan Pharmaceuticals, Inc.; Eli Lilly and Company; EuroImmun; F. Hoffmann-La Roche Ltd and its affiliated company Genentech, Inc.; Fujirebio; GE Healthcare; IXICO Ltd.; Janssen Alzheimer Immunotherapy Research & Development, LLC.; Johnson & Johnson Pharmaceutical Research & Development LLC.; Lumosity; Lundbeck; Merck & Co., Inc.; Meso Scale Diagnostics, LLC.; NeuroRx Research; Neurotrack Technologies; Novartis Pharmaceuticals Corporation; Pfizer Inc.; Piramal Imaging; Servier; Takeda Pharmaceutical Company; and Transition Therapeutics.

Supplementary materials

Supplementary material associated with this article can be found, in the online version, at doi:10.1016/j.tjpad.2025.100252.

References

[1] Scheltens P, De Strooper B, Kivipelto M, Holstege H, Chételat G, Teunissen CE, et al. Alzheimer's disease. Lancet North Am Ed 2021;397(10284):1577–90.
[2] Jack Jr CR, Andrews JS, Beach TG, Buracchio T, Dunn B, Graf A, et al. Revised criteria for diagnosis and staging of Alzheimer's disease: alzheimer's Association Workgroup. Alzheimer's Dementia 2024;20(8):5143–69.
[3] Jagust W. Imaging the evolution and pathophysiology of Alzheimer disease. Nat Rev Neurosci 2018;19(11):687–700.
[4] Sperling RA, Aisen PS, Beckett LA, Bennett DA, Craft S, Fagan AM, et al. Toward defining the preclinical stages of Alzheimer's disease: recommendations from the National Institute on Aging-Alzheimer's Association workgroups on diagnostic guidelines for Alzheimer's disease. Alzheimer's Dementia 2011;7(3):280–92.
[5] Therriault J, Schindler SE, Salvadó G, Pascoal TA, Benedet AL, Ashton NJ, et al. Biomarker-based staging of Alzheimer disease: rationale and clinical applications. Nat Rev Neurol 2024;20(4):232–44.
[6] Teunissen CE, Verberk IM, Thijssen EH, Vermunt L, Hansson O, Zetterberg H, et al. Blood-based biomarkers for Alzheimer's disease: towards clinical implementation. Lancet Neurol 2022;21(1):66–77.
[7] Yu L, Boyle PA, Janelidze S, Petyuk VA, Wang T, Bennett DA, et al. Plasma p-tau181 and p-tau217 in discriminating PART, AD and other key neuropathologies in older adults. Acta Neuropathol 2023;146(1):1–11.
[8] Thijssen EH, La Joie R, Strom A, Fonseca C, Iaccarino L, Wolf A, et al. Plasma phosphorylated tau 217 and phosphorylated tau 181 as biomarkers in Alzheimer's disease and frontotemporal lobar degeneration: a retrospective diagnostic performance study. Lancet Neurol 2021;20(9):739–52.
[9] Grothe MJ, Moscoso A, Ashton NJ, Karikari TK, Lantero-Rodriguez J, Snellman A, et al. Associations of fully automated CSF and novel plasma biomarkers with Alzheimer disease neuropathology at autopsy. Neurology 2021;97(12) e1229-e42.
[10] Morrison MS, Aparicio HJ, Blennow K, Zetterberg H, Ashton NJ, Karikari TK, et al. Ante-mortem plasma phosphorylated tau (181) predicts Alzheimer's disease neuropathology and regional tau at autopsy. Brain 2022;145(10):3546–57.
[11] Mielke MM, Frank RD, Dage JL, Jeromin A, Ashton NJ, Blennow K, et al. Comparison of plasma phosphorylated tau species with amyloid and tau positron emission tomography, neurodegeneration, vascular pathology, and cognitive outcomes. JAMA Neurol 2021;78(9):1108–17.
[12] Brum WS, Cullen NC, Therriault J, Janelidze S, Rahmouni N, Stevenson J, et al. A blood-based biomarker workflow for optimal tau-PET referral in memory clinic settings. Nat Commun 2024;15(1):2311.
[13] Palmqvist S, Janelidze S, Quiroz YT, Zetterberg H, Lopera F, Stomrud E, et al. Discriminative accuracy of plasma phospho-tau217 for Alzheimer disease vs other neurodegenerative disorders. JAMA 2020;324(8):772–81.
[14] Schindler SE, Petersen KK, Saef B, Tosun D, Shaw LM, Zetterberg H, et al. Head-to-head comparison of leading blood tests for Alzheimer's disease pathology. Alzheimer's Dementia 2024;20(11):8074–96.
[15] Barthélemy NR, Salvadó G, Schindler SE, He Y, Janelidze S, Collij LE, et al. Highly accurate blood test for Alzheimer's disease is similar or superior to clinical cerebrospinal fluid tests. Nat Med 2024;30(4):1085–95.
[16] Therriault J, Servaes S, Tissot C, Rahmouni N, Ashton NJ, Benedet AL, et al. Equivalence of plasma p-tau217 with cerebrospinal fluid in the diagnosis of Alzheimer's disease. Alzheimer's Dementia 2023;19(11):4967–77.
[17] Mendes AJ, Ribaldi F, Lathuiliere A, Ashton NJ, Janelidze S, Zetterberg H, et al. Head-to-head study of diagnostic accuracy of plasma and cerebrospinal fluid p-tau217 versus p-tau181 and p-tau231 in a memory clinic cohort. J Neurol 2024;271(4):2053–66.
[18] Sims JR, Zimmer JA, Evans CD, Lu M, Ardayfio P, Sparks J, et al. Donanemab in early symptomatic Alzheimer disease: the TRAILBLAZER-ALZ 2 randomized clinical trial. JAMA 2023;330(6):512–27.
[19] Van Dyck CH, Swanson CJ, Aisen P, Bateman RJ, Chen C, Gee M, et al. Lecanemab in early Alzheimer's disease. N Engl J Med 2023;388(1):9–21.
[20] Sperling RA, Donohue MC, Raman R, Rafii MS, Johnson K, Masters CL, et al. Trial of solanezumab in preclinical Alzheimer's disease. N Engl J Med 2023;389(12):1096–107.
[21] Devanarayan V, Charil A, Horie K, Doherty T, Llano DA, Andreozzi E, et al. Plasma pTau217 ratio predicts continuous regional brain tau accumulation in amyloid-positive early Alzheimer's disease. Alzheimer's Dementia 2024.
[22] Lowe VJ, Wiste HJ, Senjem ML, Weigand SD, Therneau TM, Boeve BF, et al. Widespread brain tau and its association with ageing, Braak stage and Alzheimer's dementia. Brain 2018;141(1):271–87.
[23] Graff-Radford J, Yong KX, Apostolova LG, Bouwman FH, Carrillo M, Dickerson BC, et al. New insights into atypical Alzheimer's disease in the era of biomarkers. Lancet Neurol 2021;20(3):222–34.

[24] Braak H, Braak E. Neuropathological stageing of Alzheimer-related changes. Acta Neuropathol 1991;82(4):239–59.
[25] Braak H, Alafuzoff I, Arzberger T, Kretzschmar H, Del Tredici K. Staging of Alzheimer disease-associated neurofibrillary pathology using paraffin sections and immunocytochemistry. Acta Neuropathol 2006;112(4):389–404.
[26] Chen X, Toueg TN, Harrison TM, Baker SL, Jagust WJ. Regional tau deposition reflects different pathways of subsequent neurodegeneration and memory decline in cognitively normal older adults. Ann Neurol 2024;95(2):249–59.
[27] Ossenkoppele R, Lyoo CH, Sudre CH, van Westen D, Cho H, Ryu YH, et al. Distinct tau PET patterns in atrophy-defined subtypes of Alzheimer's disease. Alzheimer's Dementia 2020;16(2):335–44.
[28] Ossenkoppele R, Schonhaut DR, Schöll M, Lockhart SN, Ayakta N, Baker SL, et al. Tau PET patterns mirror clinical and neuroanatomical variability in Alzheimer's disease. Brain 2016;139(5):1551–67.
[29] Chen X, Juarez A, Mason S, Kobayashi S, Baker SL, Harrison TM, et al. Longitudinal relationships between aβ and tau to executive function and memory in cognitively normal older adults. Neurobiol Aging 2025;145:32–41.
[30] Tissot C, Therriault J, Pascoal TA, Chamoun M, Lussier FZ, Savard M, et al. Association between regional tau pathology and neuropsychiatric symptoms in aging and dementia due to Alzheimer's disease. Alzheimer's Dementia: Translat Res Clin Interv 2021;7(1):e12154.
[31] Doré V, Doecke JD, Saad ZS, Triana-Baltzer G, Slemmon R, Krishnadas N, et al. Plasma p217+tau versus NAV4694 amyloid and MK6240 tau PET across the Alzheimer's continuum. Alzheimer's & Dementia: diagnosis. Assessment Disease Monitor 2022;14(1):e12307.
[32] Ferreira PC, Therriault J, Tissot C, Ferrari-Souza JP, Benedet AL, Povala G, et al. Plasma p-tau231 and p-tau217 inform on tau tangles aggregation in cognitively impaired individuals. Alzheimer's Dementia 2023;19(10):4463–74.
[33] Therriault J, Ashton NJ, Pola I, Triana-Baltzer G, Brum WS, Di Molfetta G, et al. Comparison of two plasma p-tau217 assays to detect and monitor Alzheimer's pathology. EBioMedicine 2024:102.
[34] Therriault J, Vermeiren M, Servaes S, Tissot C, Ashton NJ, Benedet AL, et al. Association of phosphorylated tau biomarkers with amyloid positron emission tomography vs tau positron emission tomography. JAMA Neurol 2023;80(2):188–99.
[35] Mundada NS, Rojas JC, Vandevrede L, Thijssen EH, Iaccarino L, Okoye OC, et al. Head-to-head comparison between plasma p-tau217 and flortaucipir-PET in amyloid-positive patients with cognitive impairment. Alzheimers Res Ther 2023;15(1):157.
[36] Ashton NJ, Brum WS, Di Molfetta G, Benedet AL, Arslan B, Jonaitis E, et al. Diagnostic accuracy of a plasma phosphorylated tau 217 immunoassay for Alzheimer disease pathology. JAMA Neurol 2024;81(3):255–63.
[37] Janelidze S, Berron D, Smith R, Strandberg O, Proctor NK, Dage JL, et al. Associations of plasma phospho-tau217 levels with tau positron emission tomography in early Alzheimer disease. JAMA Neurol 2021;78(2):149–56.
[38] Pereira JB, Janelidze S, Stomrud E, Palmqvist S, Van Westen D, Dage JL, et al. Plasma markers predict changes in amyloid, tau, atrophy and cognition in non-demented subjects. Brain 2021;144(9):2826–36.
[39] Leuzy A, Smith R, Cullen NC, Strandberg O, Vogel JW, Binette AP, et al. Biomarker-based prediction of longitudinal tau positron emission tomography in Alzheimer disease. JAMA Neurol 2022;79(2):149–58.
[40] Sperling RA, Donohue MC, Raman R, Sun C-K, Yaari R, Holdridge K, et al. Association of factors with elevated amyloid burden in clinically normal older individuals. JAMA Neurol 2020;77(6):735–45.
[41] Sperling RA, Donohue M, Rissman R, Johnson K, Rentz D, Grill J, et al. Amyloid and tau prediction of cognitive and functional decline in unimpaired older individuals: longitudinal data from the A4 and LEARN studies. J Prev Alzheimers Dis 2024;11(4):802–13.
[42] Landau SM, Lu M, Joshi AD, Pontecorvo M, Mintun MA, Trojanowski JQ, et al. Comparing positron emission tomography imaging and cerebrospinal fluid measurements of β-amyloid. Ann Neurol 2013;74(6):826–36.
[43] Rissman RA, Donohue M, Langford O, Raman R, Abdel-Latif S, Yaari R, et al. Longitudinal phospho-tau217 predicts amyloid positron emission tomography in asymptomatic Alzheimer's disease. J Prev Alzheimers Dis 2024;11(4):823–30.
[44] Arranz J, Zhu N, Rubio-Guerra S, Rodríguez-Baz Í, Ferrer R, Carmona-Iragui M, et al. Diagnostic performance of plasma pTau217, pTau181, Aβ1-42 and Aβ1-40 in the LUMIPULSE automated platform for the detection of Alzheimer disease. Alzheimers Res Ther 2024;16(1):139.
[45] Shaw LM, Korecka M, Lee EB, Cousins KA, Vanderstichele H, Schindler SE, et al. ADNI Biomarker Core: a review of progress since 2004 and future challenges. Alzheimer's Dementia 2025;21(1):e14264.
[46] Baker SL, Lockhart SN, Price JC, He M, Huesman RH, Schonhaut D, et al. Reference tissue–based kinetic evaluation of 18F-AV-1451 for tau imaging. J Nucl Med 2017;58(2):332–8.
[47] Jack Jr CR, Wiste HJ, Weigand SD, Therneau TM, Lowe VJ, Knopman DS, et al. Defining imaging biomarker cut points for brain aging and Alzheimer's disease. Alzheimer's Dementia 2017;13(3):205–16.
[48] Maass A, Landau S, Baker SL, Horng A, Lockhart SN, La Joie R, et al. Comparison of multiple tau-PET measures as biomarkers in aging and Alzheimer's disease. Neuroimage 2017;157:448–63.
[49] Lowe VJ, Lundt ES, Albertson SM, Min H-K, Fang P, Przybelski SA, et al. Tau-positron emission tomography correlates with neuropathology findings. Alzheimer's & Dementia 2019.
[50] Soleimani-Meigooni DN, Iaccarino L, La Joie R, Baker S, Bourakova V, Boxer AL, et al. 18F-flortaucipir PET to autopsy comparisons in Alzheimer's disease and other neurodegenerative diseases. Brain 2020;143(11):3477–94.
[51] Freiburghaus T, Pawlik D, Oliveira Hauer K, Ossenkoppele R, Strandberg O, Leuzy A, et al. Association of in vivo retention of [18f] flortaucipir pet with tau neuropathology in corresponding brain regions. Acta Neuropathol 2024;148(1):44.
[52] Mattsson-Carlgren N, Janelidze S, Bateman RJ, Smith R, Stomrud E, Serrano GE, et al. Soluble P-tau217 reflects amyloid and tau pathology and mediates the association of amyloid with tau. EMBO Mol Med 2021;13(6):e14022.
[53] Janelidze S, Barthélemy NR, Salvadó G, Schindler SE, Palmqvist S, Mattsson–Carlgren N, et al. Plasma phosphorylated tau 217 and Aβ42/40 to predict early brain aβ accumulation in people without cognitive impairment. JAMA Neurol 2024;81(9):947–57.
[54] Schöll M, Lockhart SN, Schonhaut DR, O'Neil JP, Janabi M, Ossenkoppele R, et al. PET imaging of tau deposition in the aging human brain. Neuron 2016;89(5):971–82.
[55] Therriault J, Pascoal TA, Lussier FZ, Tissot C, Chamoun M, Bezgin G, et al. Biomarker modeling of Alzheimer's disease using PET-based Braak staging. Nature Aging 2022;2(6):526–35.
[56] Woo MS, Therriault J, Jonaitis EM, Wilson R, Langhough RE, Rahmouni N, et al. Identification of late-stage tau accumulation using plasma phospho-tau217. EBio Medic 2024;109.
[57] Jack Jr CR, Wiste HJ, Algeciras-Schimnich A, Figdore DJ, Schwarz CG, Lowe VJ, et al. Predicting amyloid PET and tau PET stages with plasma biomarkers. Brain 2023;146(5):2029–44.
[58] Warmenhoven N, Salvadó G, Janelidze S, Mattsson-Carlgren N, Bali D, Orduña Dolado A, et al. A comprehensive head-to-head comparison of key plasma phosphorylated tau 217 biomarker tests. Brain 2024 awae346.
[59] Moloney CM, Labuzan SA, Crook JE, Siddiqui H, Castanedes-Casey M, Lachner C, et al. Phosphorylated tau sites that are elevated in Alzheimer's disease fluid biomarkers are visualized in early neurofibrillary tangle maturity levels in the post mortem brain. Alzheimer's Dementia 2023;19(3):1029–40.
[60] Groot C, Cicognola C, Bali D, Triana-Baltzer G, Dage JL, Pontecorvo MJ, et al. Diagnostic and prognostic performance to detect Alzheimer's disease and clinical progression of a novel assay for plasma p-tau217. Alzheimers Res Ther 2022;14(1):67.
[61] Janelidze S, Bali D, Ashton NJ, Barthélemy NR, Vanbrabant J, Stoops E, et al. Head–to-head comparison of 10 plasma phospho-tau assays in prodromal Alzheimer's disease. Brain 2023;146(4):1592–601.
[62] Klunk WE, Koeppe RA, Price JC, Benzinger TL, Devous Sr MD, Jagust WJ, et al. The Centiloid Project: standardizing quantitative amyloid plaque estimation by PET. Alzheimer's Dementia 2015;11(1):1–15 e4.
[63] Landau SM, Harrison TM, Baker SL, Boswell MS, Lee J, Taggett J, et al. Positron emission tomography harmonization in the Alzheimer's Disease Neuroimaging Initiative: a scalable and rigorous approach to multisite amyloid and tau quantification. Alzheimer's Dementia 2024.
[64] Vogel JW, Young AL, Oxtoby NP, Smith R, Ossenkoppele R, Strandberg OT, et al. Four distinct trajectories of tau deposition identified in Alzheimer's disease. Nat Med 2021;27(5):871–81.